Research Square

Preprints are preliminary reports that have not undergone peer review.
They should not be considered conclusive, used to inform clinical practice,
or referenced by the media as validated information.

Histological evaluation of a fully synthetic self-assembling peptide-based submucosal injection solution following cap-assisted endoscopic mucosal resection in a porcine model

Shuhei Hayasaka
Hokkaido University Graduate School of Medicine
Masayoshi Ono
cdf41180@gmail.com

Hokkaido University Graduate School of Medicine
Zijian Yang
Hokkaido University Graduate School of Medicine
Keiko Yamamoto
Hokkaido University Graduate School of Medicine
Erina Ishibe
Hokkaido University Graduate School of Medicine
Hiroki Egami
Hokkaido University Graduate School of Medicine
Sae Nakajima
Hokkaido University Graduate School of Medicine
Masayuki Higashino
Hokkaido University Graduate School of Medicine
Takayuki Sone
Hokkaido University Graduate School of Medicine
Xinhan Zhang
Hokkaido University Graduate School of Medicine
Masaki Inoue
Hokkaido University Hospital
Shuichi Miyamoto
Hokkaido University Graduate School of Medicine
Noriyuki Otsuka
Hokkaido University Hospital
Yusuke Watanabe
Hokkaido University Hospital

Naoya Sakamoto
Hokkaido University Graduate School of Medicine
Shoko Ono
Hokkaido University Hospital

Article

Keywords: self-assembling peptide hydrogel, submucosal injection solution, endoscopic mucosal resection, ulcer healing

Posted Date: November 23rd, 2026

DOI: https://doi.org/10.21203/rs.3.rs-11431986/v1

License: This work is licensed under a Creative Commons Attribution 4.0 International License.
Read Full License

Additional Declarations: No competing interests reported.

Abstract

PuraLift™, a fully synthetic self-assembling peptide-based submucosal injection solution, has been developed for endoscopic resection, but its local histological effects during ulcer healing remain unclear. Normal saline (NS), 0.6% sodium alginate (SA), and PuraLift™ were evaluated. Ex vivo, four submucosal cushions per solution were created in porcine stomach specimens; heights were measured immediately and at 5, 15, and 30 min after injection. In vivo, cap-assisted endoscopic mucosal resection (CEMR) was performed at three gastric sites in each of five pigs. Ulcer diameters were measured on days 1, 8, 15, and 22, with histological and immunohistochemical assessments on day 22. PuraLift™ produced greater initial cushion height than NS and higher cushion retention than SA and NS at 30 min. Day-8 ulcer reduction rates were significantly higher with PuraLift™ and SA than NS. On day 22, all SA sites showed residual material with foreign body giant cell reaction, whereas PuraLift™ showed no residual material and minimal foreign body giant cell reaction. Fibrotic layer thickness and CD107a- and α-smooth muscle actin-positive areas were lower with PuraLift™ than SA. PuraLift™ maintained submucosal elevation with a limited residual material-related tissue response following CEMR in a porcine model.

Introduction

Endoscopic resection, including endoscopic mucosal resection (EMR) and endoscopic submucosal dissection (ESD), is broadly employed as a standard treatment for early stage gastrointestinal tumors [1, 2]. Although these procedures are less invasive than surgical resection, procedure-related adverse events, including bleeding and perforation, remain crucial clinical concerns [3, 4].

Submucosal injection is critical for safe endoscopic resection as it forms a cushion between the lesion and the muscularis propria [5]. An ideal submucosal injection solution should offer adequate and sustained mucosal elevation, enable smooth injection through an endoscopic catheter, and have favorable biocompatibility and biodegradability without inducing local tissue toxicity [5, 6]. Various injection solutions have been developed for improving the safety and technical feasibility of endoscopic resection.

PuraLift™ (3-D Matrix, Ltd., Tokyo, Japan) is a recently developed submucosal injection solution based on self-assembling peptide hydrogel technology [7]. PuraLift™ is a 0.3% self-assembling peptide solution comprising amino acids, including arginine, alanine, and aspartic acid. PuraLift™ may have a low risk of biological contamination and favorable biocompatibility, as it is fully synthetic and does not contain animal- or human-derived components [7, 8]. Upon contact with blood or body fluids, self-assembling peptides form a three-dimensional hydrogel structure, potentially contributing to continued submucosal elevation [7].

Moreover, previous experimental studies have reported that the three-dimensional network structure of self-assembling peptide hydrogels supports cell proliferation and tissue repair [9, 10].

Therefore, PuraLift™ may offer a stable submucosal cushion during endoscopic resection and influence the local tissue response in subsequent post-resection ulcer healing. However, the histological tissue response to PuraLift™ during post-resection ulcer healing remains unclear. To our knowledge, this is the first study to comprehensively evaluate the local histological response to PuraLift™ after submucosal injection. This study aimed to evaluate the submucosal lifting performance of PuraLift™ and the histological tissue response during ulcer healing following cap-assisted EMR (CEMR) in a porcine model.

Results

Ex vivo assessment of submucosal cushion formation using resected porcine stomach specimens

The initial cushion height significantly differed among the three groups (SA, 6.1 ± 0.6 mm; PuraLift™, 7.0 ± 0.6 mm; and NS, 5.0 ± 0.2 mm; $P < 0.005$). The PuraLift™ and SA groups demonstrated a significantly greater initial cushion height than the NS group (PuraLift vs. NS, $P < 0.001$; SA vs. NS, $P < 0.05$). The PuraLift™ and SA groups showed no significant difference ($P = 0.06$) (Fig. 1).

The 5-min cushion retention rate did not significantly differ among the three groups (SA, 90.0% ± 5.3%; PuraLift™, 93.5% ± 2.7%; and NS, 85.9% ± 7.2%; $P = 0.19$). At 15 min, the cushion retention rate significantly differed among the groups (SA, 73.9% ± 2.5%; PuraLift™, 86.1% ± 6.1%; and NS, 61.1% ± 9.1%; $P < 0.005$). The PuraLift™ and SA groups exhibited significantly higher retention rates than the NS group (PuraLift™ vs. NS, $P < 0.005$; SA vs. NS, $P < 0.05$), whereas the PuraLift™ and SA groups showed no significant difference ($P = 0.06$) (Fig. 2). At 30 min, the cushion retention rate also significantly differed among the three groups (SA, 50.6% ± 7.1%; PuraLift™, 79.5% ± 5.2%; and NS, 32.3% ± 6.3%; $P < 0.001$). The PuraLift™ group demonstrated a significantly higher retention rate than the SA and NS groups (PuraLift™ vs. SA, $P < 0.001$; PuraLift™ vs. NS, $P < 0.001$). Furthermore, the SA group exhibited a significantly higher retention rate than the NS group ($P < 0.01$) (Fig. 2).

In vivo assessment of post-CEMR ulcers in the porcine stomach

All CEMR procedures were successfully completed without procedure-related complications; all five pigs completed the 22-day observation period. On day 1, the mean ulcer diameter did not significantly differ among the three groups (PuraLift™, 10.6 ± 3.8 mm; SA, 9.2 ± 3.3 mm; and NS, 9.4 ± 2.4 mm; $P = 0.76$). Of the 15 post-CEMR ulcers, 13 demonstrated macroscopic closure by day 22, whereas 2 in the NS group remained open.

Ulcer reduction rate

The ulcer reduction rate was evaluated on days 8, 15, and 22 (Fig. 3).

On day 8, the ulcer reduction rate significantly differed among the three groups (PuraLift™, 19.3% ± 15.9%; SA, 19.7% ± 19.2%; and NS, − 10.5% ± 14.4%; $P < 0.05$). The PuraLift™ and SA groups exhibited significantly higher ulcer reduction rates than the NS group (PuraLift™ vs. NS, $P < 0.05$; SA vs. NS, $P < 0.05$), whereas no significant difference was noted between the PuraLift™ and SA groups ($P = 0.99$).

On day 15, the ulcer reduction rate did not significantly differ among the three groups (PuraLift™, 75.6% ± 7.7%; SA, 61.6% ± 25.9%; and NS, 41.7% ± 30.7%; $P = 0.11$). Similarly, no significant difference was observed on day 22 (PuraLift™, 100.0% ± 0.0%; SA, 100.0% ± 0.0%; and NS, 92.6% ± 11.1%; $P = 0.15$).

Ulcer epithelialization, residual submucosal foreign material, and foreign body giant cell reaction

On day 22, histological epithelialization, residual submucosal foreign material, and foreign body giant cell reaction were evaluated using H&E staining (Fig. 4).

All cases in the PuraLift™ group demonstrated complete epithelialization. By contrast, three cases in the NS group and one case in the SA group exhibited incomplete epithelialization (Figs. 4a–c).

All five cases in the SA group exhibited residual injection material in the submucosal layer, accompanied by a foreign body giant cell reaction. By contrast, the PuraLift™ group demonstrated no residual injection material. Furthermore, the PuraLift™ group showed minimal foreign body giant cell reaction (Figs. 4d–f).

The mean number of foreign body giant cells per high-power field significantly differed among the three groups (SA, 16.8 ± 2.5; PuraLift™, 0.4 ± 0.3; and NS, 0.4 ± 0.8; $P < 0.001$). The SA group showed a significantly higher number of foreign body giant cells than the PuraLift™ and NS groups (both $P < 0.001$), whereas no significant difference was noted between the PuraLift™ and NS groups ($P = 0.99$) (Fig. 4g).

Fibrotic layer thickness and tissue damage

The fibrotic layer thickness significantly differed among the three groups (SA, 3.7 ± 1.2 mm; PuraLift™, 1.6 ± 0.4 mm; and NS, 2.0 ± 1.0 mm; $P < 0.01$) (Fig. 5).

The SA group exhibited a significantly thicker fibrotic layer than the PuraLift™ and NS groups (SA vs. PuraLift™, $P < 0.05$; SA vs. NS, $P < 0.05$) (Fig. 5). The PuraLift™ and NS groups demonstrated no significant difference ($P = 0.81$). No tissue damage in the muscularis propria was noted in any group.

Immunohistochemical analysis

The mean CD107a-positive staining area, used as an indicator of macrophage accumulation, significantly differed among the three groups (SA, 15.4% ± 3.7%; PuraLift™, 5.0% ± 2.5%; and NS, 1.2% ± 1.9%; $P < 0.001$) (Fig. 6a). The SA group demonstrated significantly greater CD107a-positive staining

than the PuraLift™ and NS groups (SA vs. PuraLift™, P < 0.001; SA vs. NS, P < 0.001). No significant difference was noted between the PuraLift™ and NS groups (P = 0.12).

The mean α-SMA–positive staining area, used as an indicator of myofibroblast accumulation, also significantly differed among the three groups (SA, 26.4% ± 2.8%; PuraLift™, 10.5% ± 2.2%; and NS, 17.6% ± 6.5%; P < 0.001) (Fig. 6b).

The SA group exhibited significantly greater α-SMA–positive staining than the PuraLift™ and NS groups (SA vs. PuraLift™, P < 0.001; SA vs. NS, P < 0.05). No significant difference was noted between the PuraLift™ and NS groups (P = 0.06).

By contrast, the mean CD3-positive staining area did not significantly differ among the three groups (SA, 0.12% ± 0.08%; PuraLift™, 0.02% ± 0.02%; and NS, 0.09% ± 0.11%; P = 0.16) (Fig. 6c).

Similarly, the mean CD31-positive staining area did not significantly differ among the groups (SA, 3.3% ± 1.8%; PuraLift™, 3.1% ± 1.1%; and NS, 2.4% ± 1.1%; P = 0.59) (Fig. 6d).

Discussion

This study revealed that PuraLift™ offered sustained submucosal elevation and was associated with limited residual material-related tissue reaction following CEMR in a porcine model.

Ex vivo assessment indicated that PuraLift™ provided greater initial submucosal elevation than NS and showed a more sustained elevation at 15 and 30 min. Moreover, it exhibited a higher cushion retention rate than SA at 30 min. Sustained mucosal elevation is crucial for maintaining separation between the target lesion and the muscularis propria during endoscopic resection. Under physiological conditions, self-assembling peptides form nanofibers and three-dimensional networks and undergo local gelation following injection [12]. The favorable lifting performance of PuraLift™ observed in the *ex vivo* model may be attributed to this gel-forming property.

Next, we evaluated post-CEMR ulcer healing in an *in vivo* porcine model. On day 22, all cases in the SA group exhibited residual injection material in the submucosal layer, accompanied by a foreign body giant cell reaction. Furthermore, the SA group demonstrated greater CD107a- and α-SMA–positive staining areas and a thicker fibrotic layer than the other groups. By contrast, the PuraLift™ group showed no apparent residual foreign material, and the foreign body giant cell reaction was minimal. Additionally, the CD107a- and α-SMA–positive staining areas and fibrotic layer thickness did not significantly differ between the PuraLift™ and NS groups. These results suggest an association between PuraLift™ and limited material-related tissue reaction in this porcine model.

In this study, SA was used as a conventional alginate-based comparator. Although alginate is generally considered biocompatible, various factors, including purity, formulation, viscosity, injection site, and persistence of residual material, can influence its local tissue response [13, 14]. Foreign body reactions

or fibrosis following alginate implantation have been reported in other biomedical applications, such as hemostatic materials, implanted alginate spheres, and wound dressings [15, 16, 17, 18].

In general, persistent foreign material can prompt macrophage recruitment and foreign body giant cell formation, causing myofibroblast accumulation and fibrotic tissue response through inflammatory and profibrotic mediators [19, 20]. Therefore, the greater foreign body giant cell reaction and fibrotic layer thickness noted in the SA group may reflect a persistent tissue response associated with residual injection material in this model.

PuraLift™ is a fully synthetic peptide solution comprising amino acids naturally present in the human body. Its biodegradability may have enabled earlier degradation and clearance from the tissue, thereby restricting residual material-associated persistent foreign body reaction and fibrotic tissue response. However, this study indirectly assessed the degradation process of PuraLift™; further studies are warranted to elucidate its temporal behavior in the submucosal layer.

The PuraLift™ and SA groups demonstrated significantly higher ulcer reduction rates on day 8 than the NS group. Early ulcer size reduction may reflect favorable wound healing; however, enhanced wound contraction associated with local tissue reaction may also influence this reduction. In the PuraLift™ group, the three-dimensional network structure of the self-assembling peptide hydrogel may have supported early ulcer size reduction by providing a scaffold-like environment for cell proliferation [12, 21]. However, this study did not directly assess epithelial cell proliferation or molecular mechanisms of tissue repair. Therefore, whether PuraLift™ directly promoted wound healing remains uncertain. In the SA group, early ulcer size reduction may have been associated with physical protection or scaffold-like effects of the residual gel material; however, it may also have reflected wound contraction linked to foreign body reaction and fibrotic tissue response.

The clinical impact of material-related local tissue reactions, including inflammation, foreign body reaction, and fibrosis, following endoscopic resection remains controversial. However, extensive mucosal defects following endoscopic resection in the gastrointestinal tract can cause luminal deformity or stricture through scar contraction and fibrosis [22]. Post-resection strictures occasionally necessitate endoscopic balloon dilation or other interventions [23, 24, 25]. Residual material-related reactions have also been documented following the clinical use of submucosal lifting agents. For example, ORISE gel, a submucosal lifting agent previously used clinically for endoscopic resection, has been demonstrated to persist in tissues and trigger foreign body reaction, granuloma formation, or local deformity following endoscopic treatment [26, 27]. Although this study employed a relatively small EMR ulcer model and did not evaluate stricture formation, minimizing residual material-related local tissue reactions may be crucial for submucosal injection solutions used in endoscopic resection. The limited residual material-related tissue reaction observed with PuraLift™ may represent an advantage during post-endoscopic resection ulcer healing. Whether this histological profile is associated with a mitigated risk of scar-related deformity or stricture requires further studies.

This study had several limitations. First, this study had a small sample size. Second, this was an animal study, and the findings may not be directly extrapolated to humans. Third, the *ex vivo* submucosal injection model could not fully reproduce *in vivo* conditions, including blood flow, body temperature, gastric juice exposure, and gastric motility. Fourth, this study evaluated post-EMR ulcers, which are generally smaller than those following ESD. As ulcer size may impact the amount of residual material and the degree of foreign body reaction, the findings may vary in larger ESD-induced ulcers. Fifth, the observation period was limited to 22 days, and longer term tissue responses were not evaluated. Finally, molecular analyses were not performed. To evaluate the safety and efficacy of PuraLift™ as a submucosal injection solution, further clinical studies are warranted.

In conclusion, to our knowledge, this is the first study to histologically evaluate the tissue response to a self-assembling peptide-based submucosal injection solution following EMR in a porcine model. PuraLift™ demonstrated favorable submucosal lifting performance and was associated with no apparent residual material, limited foreign body giant cell reaction, and restricted fibrotic response. These findings suggest that PuraLift™ can offer sustained submucosal lifting with limited residual material-related tissue reaction during post-EMR ulcer healing.

Methods

Injection materials

The following injection materials were evaluated: normal saline (NS) as the control solution, 0.6% sodium alginate (SA; Liftal K, Kaigen Pharma Co., Ltd., Osaka, Japan) as a conventional submucosal injection solution, and PuraLift™ (3-D Matrix, Ltd., Tokyo, Japan) as a fully synthetic self-assembling peptide-based solution.

Animals

Five 15–20-kg female pigs were obtained from Sankyo Labo Service (Tokyo, Japan). The Animal Care and Use Committee of Hokkaido University approved the experimental protocol. All animal experiments were conducted following the Japanese Act on Welfare and Management of Animals and institutional guidelines for the care and use of laboratory animals. This study is reported in accordance with the ARRIVE guidelines.

Ex vivo assessment of submucosal cushion formation

For the *ex vivo* assessment of submucosal cushion formation, a fresh resected stomach specimen obtained from one of the five pigs was used. The stomach was divided into three specimens, each approximately 20 × 5 cm in size. Each specimen was flattened and fixed on a rubber plate using pins. Using a 5-mL syringe with a 24-gauge needle (Terumo, Tokyo, Japan), 1 mL of each injection material was delivered from the mucosal surface into the submucosal layer. Each specimen was assigned to one injection material; four submucosal cushions were developed at 4-cm intervals. The submucosal cushions were observed from a lateral view and recorded using a digital camera immediately following

injection and at 5, 15, and 30 min thereafter. Captured images were analyzed using ImageJ software (National Institutes of Health, Bethesda, MD, USA); the height of each submucosal cushion from the mucosal surface was measured. The cushion retention rate at each time point was calculated as follows:

Cushion retention rate (%) = (cushion height at each time point [mm]/cushion height immediately following injection [mm]) × 100.

The initial cushion height immediately following injection and the cushion retention rates at 5, 15, and 30 min following injection were evaluated.

In vivo CEMR experiment for post-resection ulcer assessment

The in vivo CEMR experiments used the same five pigs. Atropine (1 mg; Terumo, Tokyo, Japan) was administered intramuscularly as a premedication. General anesthesia was induced via intramuscular administration of midazolam (4 mg; Astellas Pharma, Tokyo, Japan), butorphanol (2 mg; Meiji Seika Pharma, Tokyo, Japan), and dexmedetomidine (0.8 mg; Nippon Zenyaku Kogyo, Fukushima, Japan). Subsequently, the animals were intubated and mechanically ventilated with 3% sevoflurane in oxygen. Heart rate, cardiac activity on three-lead electrocardiography, and oxygen saturation were continuously monitored during the endoscopic procedures. Following CEMR, the animals were allowed oral fluids on the day following the procedure and solid food thereafter. In each stomach, 3 mL of each injection material (NS, SA, and PuraLift™) was injected into the submucosal layer at three separate sites using a 25-gauge injection needle (Top Co., Tokyo, Japan). CEMR was performed using a 15-mm disposable electrosurgical snare (SnareMaster; Olympus, Tokyo, Japan), a single-channel endoscope (GIF-Q240; Olympus) fitted with a transparent distal attachment cap (Olympus), and an electrosurgical generator (ESG-100; Olympus). Two endoscopists (Z.Y. and S.H.) performed all procedures (Supplementary Fig. S1). The ulcer diameter was measured endoscopically immediately following CEMR (day 1) and on days 8 and 15 using a measuring device (M2-3U; Olympus, Tokyo, Japan). On day 22, all pigs were euthanized by intravenous administration of 20 mL of 15% potassium chloride (Terumo, Tokyo, Japan) under general anesthesia. En bloc gastrectomy was then performed. The ulcer diameter was measured macroscopically; the resected stomachs underwent further histological analysis (Supplementary Fig. S1).

The ulcer reduction rate was calculated as follows:

Ulcer reduction rate (%) = ([ulcer diameter on day 1] − [ulcer diameter on each observation day])/[ulcer diameter on day 1] × 100.

Ulcer reduction rates were evaluated on days 8, 15, and 22 (Supplementary Fig. S2).

Histopathological assessment

The resected stomachs were fixed in 10% formalin, embedded in paraffin, and sectioned at a 5-μm thickness along the maximum diameter of each post-CEMR ulcer or scar. Tissue sections were evaluated using hematoxylin and eosin (H&E) staining, Masson's trichrome staining, and immunohistochemical staining for α-smooth muscle actin (α-SMA), CD107a, CD3, and CD31.

The epithelialization of the ulcer, the presence of residual foreign material in the submucosal layer, and the degree of foreign body giant cell reaction were assessed using H&E staining.

Foreign body giant cells were defined as enlarged cells with abundant cytoplasm containing ≥ 10 nuclei/cell [11].

Foreign body giant cells were counted in five randomly selected high-power fields per section at ×400 magnification using NDP.view2 software (Hamamatsu Photonics K.K., Hamamatsu, Japan) and ImageJ software (National Institutes of Health).

The mean number of foreign body giant cells per field was subsequently computed.

Masson's trichrome staining was employed for evaluating tissue damage in the muscularis propria and measuring the fibrotic layer thickness (Supplementary Fig. S3).

Immunohistochemical staining was performed using anti-α-SMA antibody (clone 1A4, dilution 1:1,000; Sigma-Aldrich, St. Louis, MO, USA) for 60 min, anti-CD107a antibody (clone 4E9/11, dilution 1:300; AbD Serotec, Kidlington, UK) for 60 min, anti-CD3 antibody (clone CD3-12, dilution 1:1,000; Bio-Rad, Hercules, CA, USA) for 60 min, and anti-CD31 antibody (M-20, dilution 1:600; Santa Cruz Biotechnology, Dallas, TX, USA) for 30 min at 25°C.

For each sample, five randomly selected fields were captured at ×400 magnification. ImageJ software (National Institutes of Health) and NDP.view2 software (Hamamatsu Photonics K.K.) were used for calculating the average positive staining areas for α-SMA, CD107a, CD3, and CD31. A gastroenterologist (S.H.) performed all histological evaluations under the supervision of a pathologist (N.O.).

Statistical analysis

All statistical analyses were conducted using GraphPad Prism version 11.0.2 (GraphPad Software, Boston, MA, USA). Continuous variables were expressed as means ± standard deviations. Comparisons among the three groups were performed using one-way analysis of variance. When a significant difference was detected, post-hoc pairwise comparisons were performed using Tukey's multiple comparisons test. A two-sided P value of < 0.05 was considered statistically significant.

Abbreviations

ANOVA	Analysis of variance
CEMR	Cap-assisted endoscopic mucosal resection

EMR	Endoscopic mucosal resection
ESD	Endoscopic submucosal dissection
H&E	Hematoxylin and eosin
NS	Normal saline
SA	Sodium alginate
SAP	Self-assembling peptide
SD	Standard deviation

Declarations

Data availability

The data supporting the findings of this study are available from the corresponding author upon reasonable request.

Acknowledgements

None.

Funding

None.

Author contributions

Data Curation (Lead), Investigation (Lead), Writing–Original Draft (Lead): Shuhei Hayasaka; Data Curation (Lead), Investigation (Lead), Writing–Review & Editing (Supporting): Zijian Yang, Keiko Yamamoto, and Yusuke Watanabe; Data Curation (Supporting), Writing–Original Draft (Supporting): Erina Ishibe, Hiroki Egami, Sae Nakajima, Masayuki Higashino, Takayuki Sone, Xinhan Zhang, Masaki Inoue, and Shuichi Miyamoto; Data Curation (Lead): Noriyuki Otsuka; Supervision (Supporting), Writing–Review & Editing (Supporting): Naoya Sakamoto, Shoko Ono; Conceptualization (Lead), Writing–Original Draft (Lead), Writing–Review & Editing (Lead), Final Approval: Masayoshi Ono

Additional information

Competing interests

Masayoshi Ono, Shoko Ono, and Shuhei Hayasaka received a supply of PuraLift™ from 3-D Matrix Ltd., Tokyo, Japan. The other authors declare no competing interests.

References

1. Pimentel-Nunes, P. et al. Endoscopic submucosal dissection: European Society of Gastrointestinal Endoscopy (ESGE) Guideline. *Endoscopy* **47**, 829–854 (2015).
2. ASGE Standards of Practice Committee. American Society for Gastrointestinal Endoscopy guideline on endoscopic submucosal dissection for the management of early esophageal and gastric cancers: summary and recommendations. *Gastrointest. Endosc*. **98**, 271–284 (2023).
3. Park, Y. M., Cho, E., Kang, H. Y. & Kim, J. M. The effectiveness and safety of endoscopic submucosal dissection compared with endoscopic mucosal resection for early gastric cancer: a systematic review and metaanalysis. *Surg. Endosc*. **25**, 2666–2677 (2011).
4. Lian, J., Chen, S., Zhang, Y. & Qiu, F. A meta-analysis of endoscopic submucosal dissection and EMR for early gastric cancer. *Gastrointest. Endosc*. **76**, 763–770 (2012).
5. Uraoka, T., Saito, Y., Yamamoto, K. & Fujii, T. Submucosal injection solution for gastrointestinal tract endoscopic mucosal resection and endoscopic submucosal dissection. *Drug Des. Devel Ther.* **2**, 131–138 (2008).
6. Ferreira, A. O., Moleiro, J., Torres, J. & Dinis-Ribeiro, M. Solutions for submucosal injection in endoscopic resection: a systematic review and meta-analysis. *Endosc Int. Open.* **4**, E1–E16 (2016).
7. Nakata, K. et al. The feasibility of a fully synthetic and self-assembled peptide solution as submucosal injection material: a preliminary animal study. *Scand. J. Gastroenterol.* **56**, 984–989 (2021).
8. Kasuga, K. et al. A novel submucosal injection material comprising a fully synthetic and self-assembling peptide solution for endoscopic resection of large colorectal laterally spreading tumors. *Endoscopy* **55**, E621–E622 (2023).
9. Kumar, D. et al. Peptide hydrogels—a tissue engineering strategy for the prevention of oesophageal strictures. *Adv. Funct. Mater.* **27**, 1702424 (2017).
10. Li, S. et al. Self-assembled peptide hydrogels in regenerative medicine. *Gels* **9**, 653 (2023).
11. ten Harkel, B. et al. The foreign body giant cell cannot resorb bone, but dissolves hydroxyapatite like osteoclasts. *PLoS ONE*. **10**, e0139564 (2015).
12. Hellmund, K. S. & Koksch, B. Self-assembling peptides as extracellular matrix mimics to influence stem cell's fate. *Front. Chem.* **7**, 172 (2019).
13. Dusseault, J. et al. Evaluation of alginate purification methods: effect on polyphenol, endotoxin, and protein contamination. *J. Biomed. Mater. Res. A*. **76**, 243–251 (2006).
14. Lee, K. Y. & Mooney, D. J. Alginate: properties and biomedical applications. *Prog Polym. Sci.* **37**, 106–126 (2012).
15. Odell, E. W., Oades, P. & Lombardi, T. Symptomatic foreign body reaction to haemostatic alginate. *Br. J. Oral Maxillofac. Surg.* **32**, 178–179 (1994).
16. Bochenek, M. A. et al. Alginate encapsulation as long-term immune protection of allogeneic pancreatic islet cells transplanted into the omental bursa of macaques. *Nat. Biomed. Eng.* **2**, 810–

821 (2018).
17. Fath-Bayati, L. & Ai, J. Assessment of mesenchymal stem cell effect on foreign body response induced by intraperitoneally implanted alginate spheres. *J. Biomed. Mater. Res. A*. **108**, 94–102 (2020).
18. Matthew, I. R., Browne, R. M., Frame, J. W. & Millar, B. G. Subperiosteal behaviour of alginate and cellulose wound dressing materials. *Biomaterials* **16**, 275–278 (1995).
19. Anderson, J. M., Rodriguez, A. & Chang, D. T. Foreign body reaction to biomaterials. *Semin Immunol.* **20**, 86–100 (2008).
20. Li, R. et al. Macrophages and fibroblasts in foreign body reactions: how mechanical cues drive cell functions? *Mater. Today Bio*. **22**, 100783 (2023).
21. Holmes, T. C. et al. Extensive neurite outgrowth and active synapse formation on self-assembling peptide scaffolds. *Proc. Natl. Acad. Sci. U.S.A.* 97, 6728–6733 (2000).
22. Iwata, K., Mikami, Y., Kato, M., Yahagi, N. & Kanai, T. Pathogenesis and management of gastrointestinal inflammation and fibrosis: from inflammatory bowel diseases to endoscopic surgery. *Inflamm. Regen*. **41**, 21 (2021).
23. Kadota, T. et al. Prophylactic steroid administration for strictures after endoscopic resection of large superficial esophageal squamous cell carcinoma. *Endosc Int. Open.* **4**, E1267–E1274 (2016).
24. Kishida, Y. et al. Effects of steroid use for stenosis prevention after wide endoscopic submucosal dissection for gastric neoplasm. *Surg. Endosc*. **32**, 751–759 (2018).
25. Takahashi, H. et al. Risk of perforation during dilation for esophageal strictures after endoscopic resection in patients with early squamous cell carcinoma. *Endoscopy* **43**, 184–189 (2011).
26. Colak, Y. et al. Potential clinical complications of Orise™ gel use, a new submucosal lifting agent: experience from a tertiary care center and review of the literature. *Ann. Gastroenterol.* **35**, 407–413 (2022).
27. Alipouriani, A. et al. Adverse tissue reactions to ORISE gel during endoscopic mucosal resection and dissection. *J. Gastrointest. Surg.* **28**, 1963–1969 (2024).

Figures

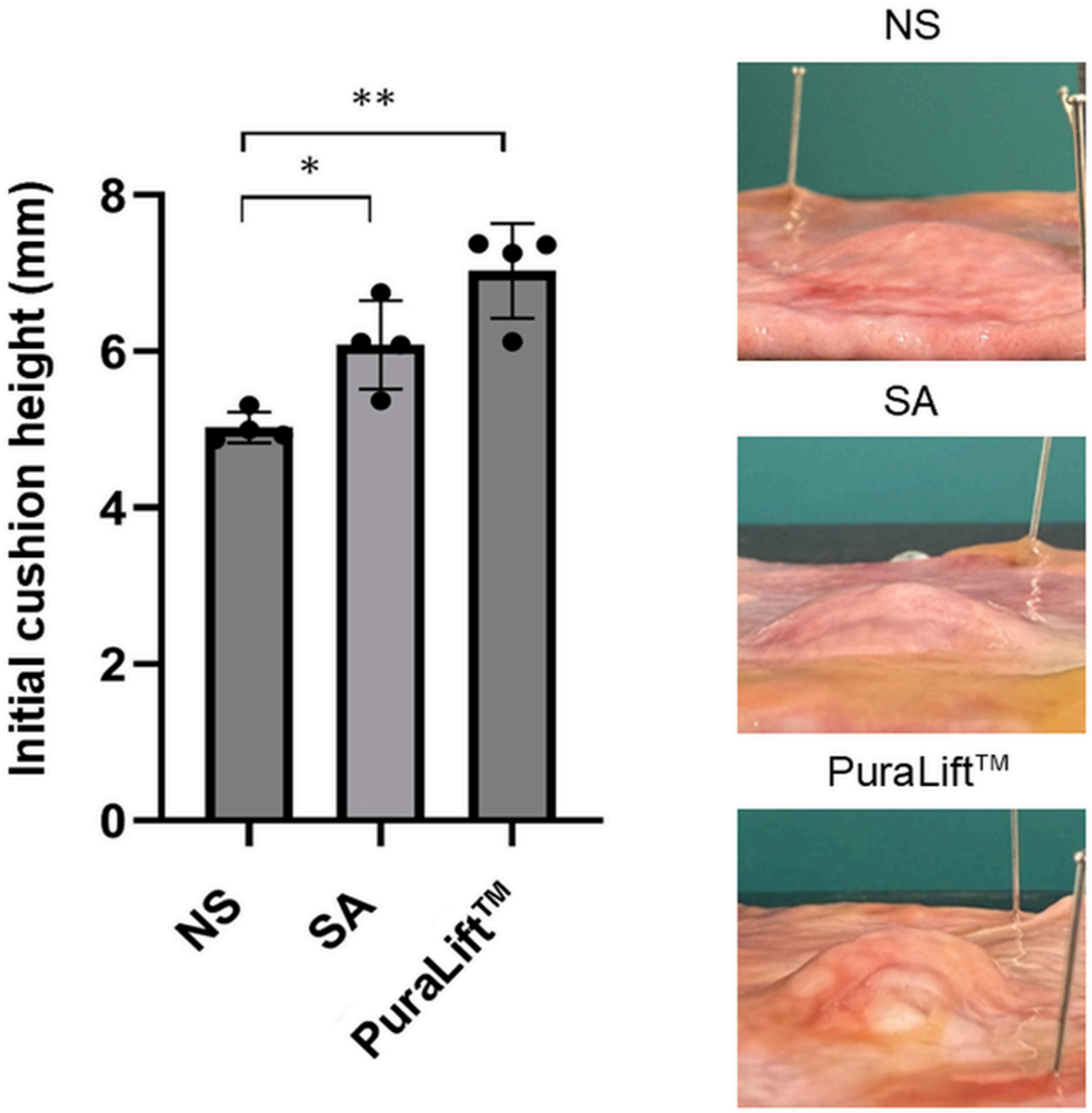

Figure 1

Initial submucosal cushion height following injection of each solution

The PuraLift™ and sodium alginate (SA) groups show significantly greater initial cushion height than the normal saline (NS) group, with the PuraLift™ and SA groups exhibiting no significant difference. Data are presented as means ± standard deviations (SDs). **P < 0.001; *P < 0.05

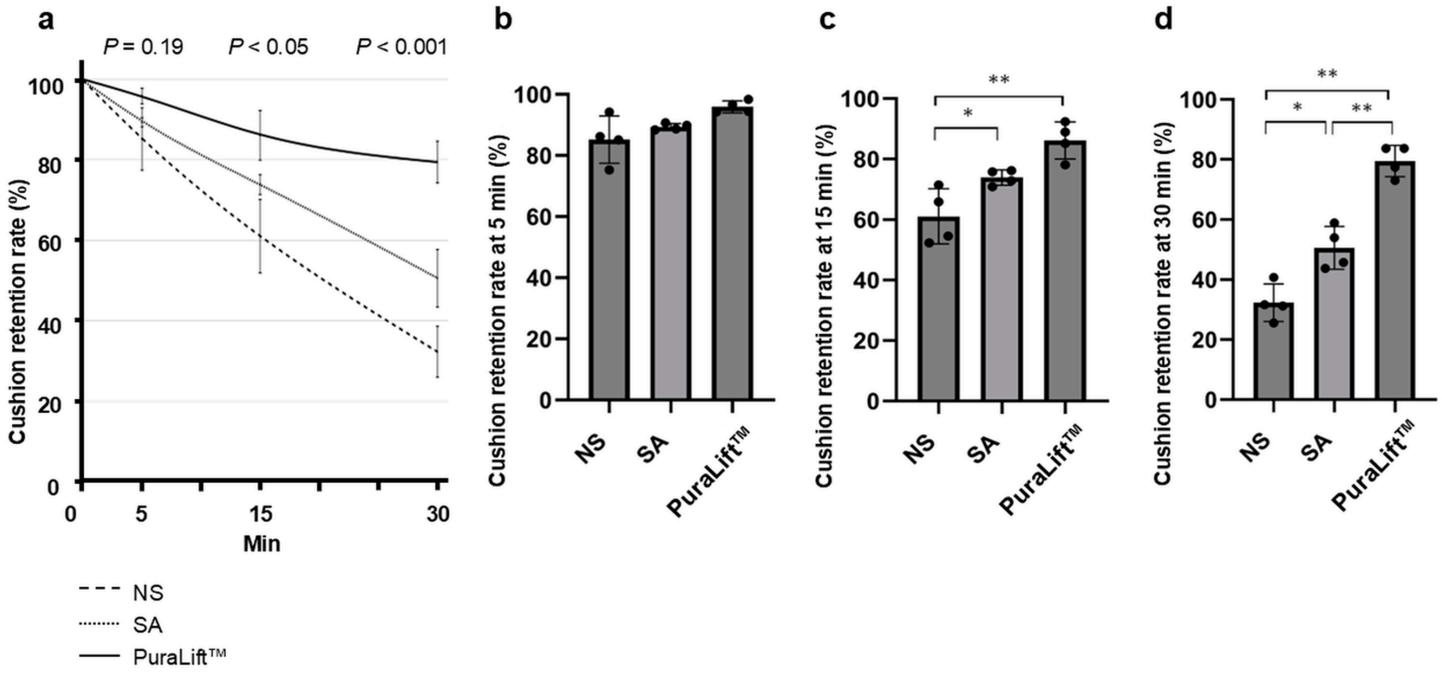

Figure 2

Cushion retention rate following injection of each solution

(a) Cushion retention rate over time following submucosal injection

(b) Cushion retention rate at 5 min. No significant difference is noted among the three groups

(c) Cushion retention rate at 15 min. The PuraLift™ and SA groups demonstrate significantly higher retention rates than the NS group, with the PuraLift™ and SA groups showing no significant difference. **P < 0.005; *P < 0.05

(d) Cushion retention rate at 30 min. The PuraLift™ group exhibits a significantly higher retention rate than the SA and NS groups; the SA group shows a significantly higher retention rate than the NS group. **P < 0.001; *P < 0.01

Data are presented as means ± SDs

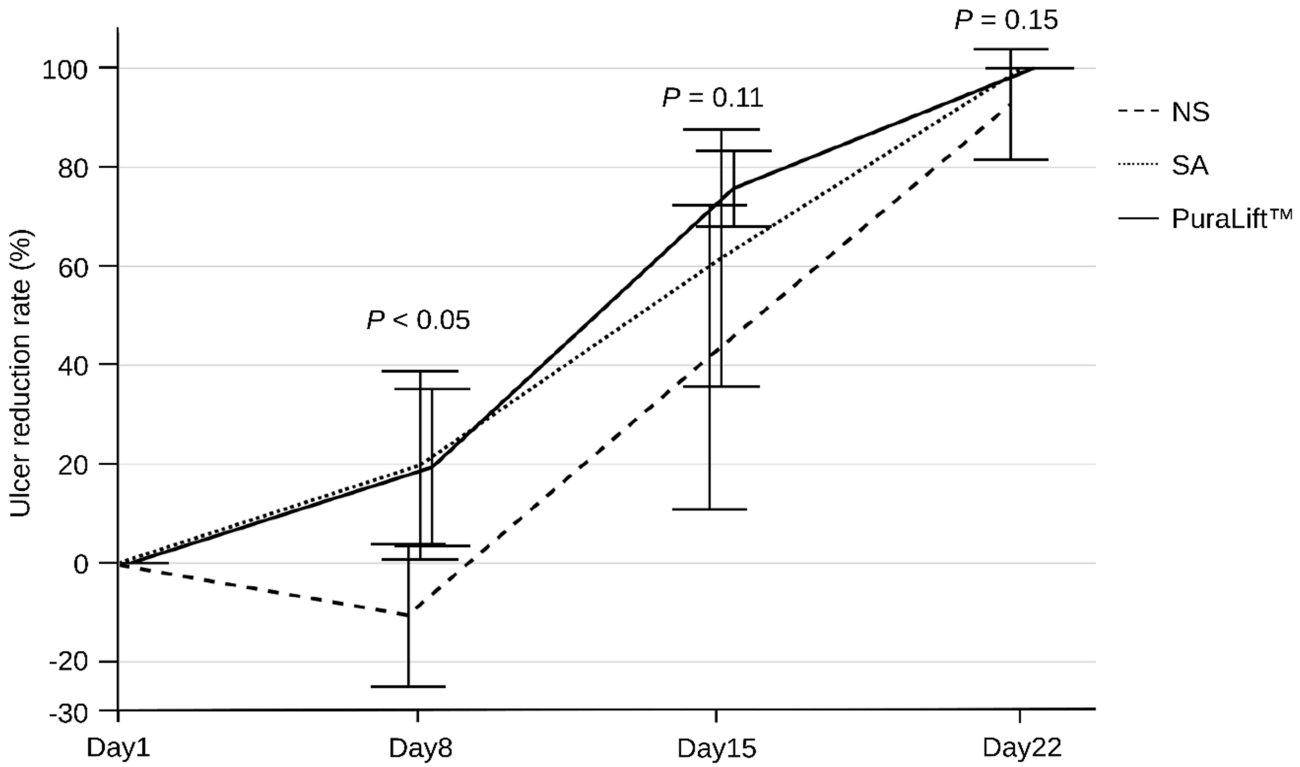

Figure 3

Ulcer reduction rate following cap-assisted endoscopic mucosal resection (CEMR)

Ulcer reduction rates are evaluated on days 8, 15, and 22. On day 8, the PuraLift™ and SA groups show significantly higher ulcer reduction rates than the NS group, with the PuraLift™ and SA groups demonstrating no significant difference. No significant differences are noted among the three groups on days 15 or 22. Data are presented as means ± SDs

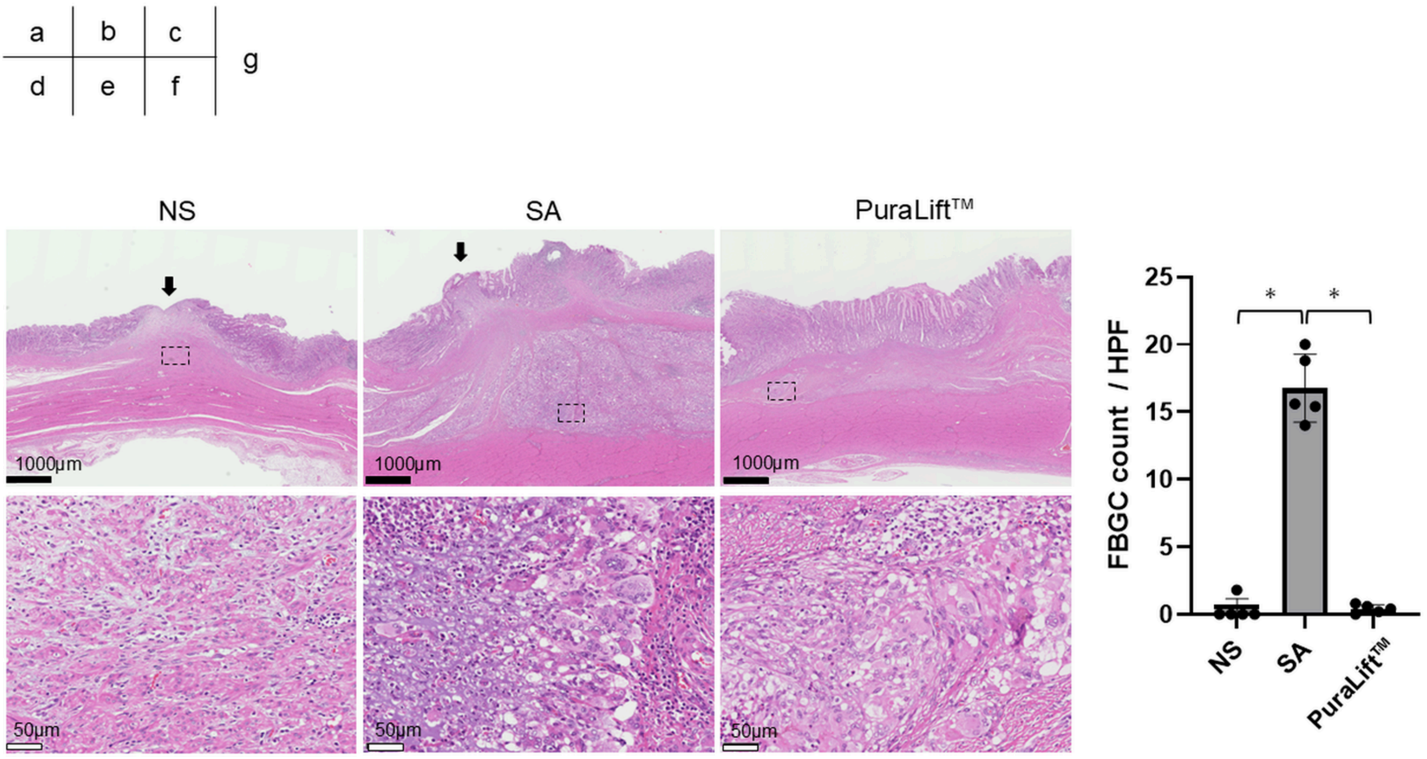

Figure 4

Ulcer epithelialization and residual submucosal foreign material on day 22

Hematoxylin and eosin-stained images of ulcer epithelialization on day 22 are shown in the upper panels (a, NS; b, SA; and c, PuraLift™). All cases in the PuraLift™ group exhibit complete epithelialization post-endoscopic mucosal resection, whereas three cases in the NS group and one case in the SA group show incomplete epithelialization (arrows in a and b). Representative images of the submucosal layer are depicted in the lower panels (d, NS; e, SA; and f, PuraLift™), corresponding to the black dotted boxes in the upper panels. All five cases in the SA group demonstrate residual injection material in the submucosal layer with foreign body giant cell reaction (e). By contrast, the PuraLift™ group exhibit no residual injection material and only minimal foreign body giant cell reaction (f). (g) Comparison of foreign body giant cells per high-power field. Data are presented as means ± SDs. *P < 0.001

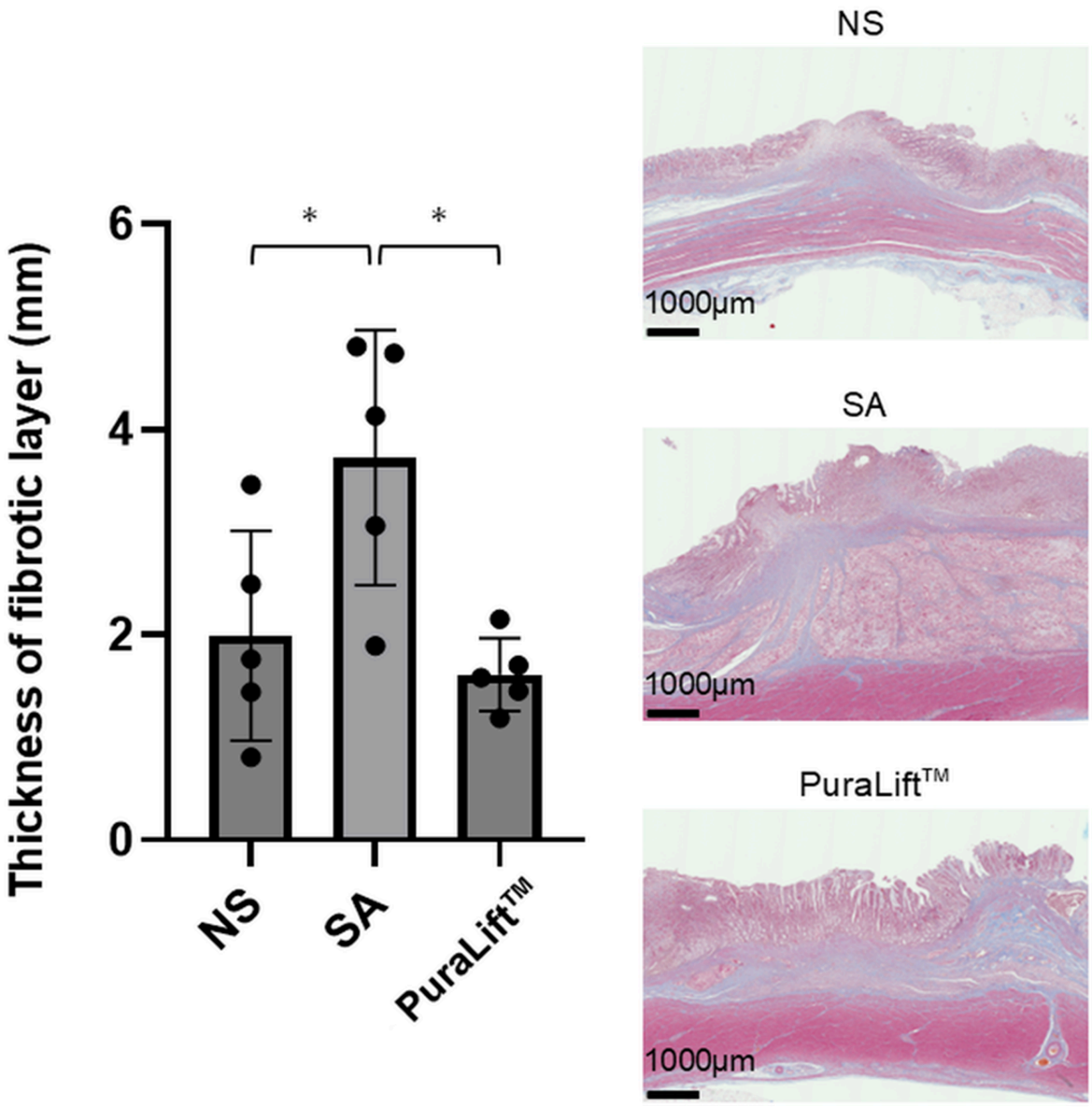

Figure 5

Fibrotic layer thickness on day 22

The SA group demonstrates a significantly thicker fibrotic layer than the PuraLift™ and NS groups, with no significant difference noted between the PuraLift™ and NS groups. No tissue damage in the muscularis propria is noted in any group. Data are presented as means ± SDs. *P < 0.05

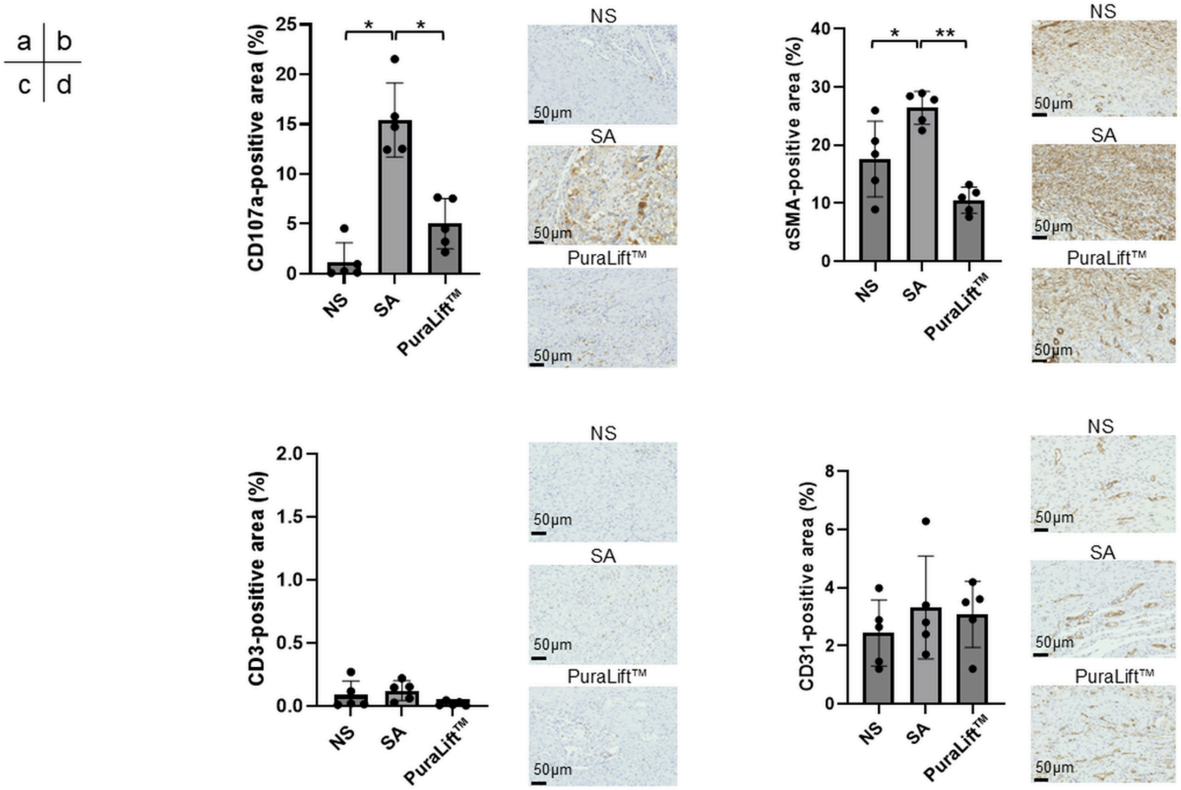

Figure 6

Immunohistochemical analysis of post- cap-assisted endoscopic mucosal resection ulcers on day 22

(a) CD107a-positive staining area is used as a macrophage accumulation indicator. The SA group shows significantly greater CD107a-positive staining than the PuraLift™ and NS groups, with no significant difference observed between the PuraLift™ and NS groups. *P < 0.001

(b) α-SMA–positive staining area is used as a myofibroblast accumulation indicator. The SA group exhibits significantly greater α-SMA–positive staining than the PuraLift™ and NS groups, with no significant difference noted between the PuraLift™ and NS groups. **P < 0.001; *P < 0.05

(c) CD3-positive staining area. No significant difference was observed among the three groups

(d) CD31-positive staining area. No significant difference was observed among the three groups

Data are presented as mean ± SD

Supplementary Files

This is a list of supplementary files associated with this preprint. Click to download.

- SupplementaryInformationScientificReports20261018.pdf